Published in final edited form as:
Cancer Discov. 2014 August ; 4(8): 942–955. doi:10.1158/2159-8290.CD-13-0873.

PTEN-DEFICIENT TUMORS DEPEND ON AKT2 FOR MAINTENANCE AND SURVIVAL

Y. Rebecca Chin[1], **Xin Yuan**[2], **Steven P. Balk**[2], and **Alex Toker**[1]

[1]Department of Pathology, Beth Israel Deaconess Medical Center, Harvard Medical School, Boston, MA

[2]Hematology-Oncology Division, Department of Medicine, Beth Israel Deaconess Medical Center, Harvard Medical School, Boston, MA

Abstract

Loss of PTEN is a common event in many cancers and leads to hyperactivation of the PI 3-K/Akt signaling pathway. The mechanisms by which Akt isoforms mediate signaling to phenotypes associated with PTEN-inactivation in cancer have not been defined. Here we show that Akt2 is exclusively required for PTEN-deficient prostate tumor spheroid maintenance whereas Akt1 is dispensable. shRNA silencing of Akt2 but not Akt1 promotes regression of prostate cancer xenografts. Mechanistically, we show that Akt2 silencing up-regulates p21 and the pro-apoptotic protein Bax and downregulates the insulin-like growth factor receptor-1. We also show that p21 is an effector of Akt2 in mediating prostate tumor maintenance. Moreover, Akt2 is also exclusively required for the maintenance and survival of other PTEN-deficient solid tumors, including breast cancer and glioblastoma. These findings identify a specific function for Akt2 in mediating survival of PTEN-deficient tumors and provide a rationale for developing therapeutics targeting Akt2.

Introduction

The phosphoinositide 3-kinase (PI 3-K) signaling pathway is frequently deregulated in virtually all human solid tumors (1). Upon activation by growth factors, class IA PI 3-Kinases phosphorylate phosphatidylinositol-4,5-bisphosphate (PIP_2) at the plasma membrane to generate phosphatidylinositol-3,4,5-trisphosphate (PIP_3) (2). PIP_3 fulfills an essential second messenger role by recruiting inactive signaling proteins to the plasma membrane, resulting in the activation of numerous pathways that transduce the signal to a plethora of cellular processes (3). The intracellular levels of PIP_3 are tightly regulated by the opposing activities of PI 3-K and phosphatase and tensin homolog (PTEN), a PIP_3 3′-phosphatase that dephosphorylates PIP_3 back to PIP_2 (4, 5). The p110α catalytic subunit of PI 3-K, encoded by the *PIK3CA* gene, is frequently activated by somatic mutation in many epithelial cancers, including breast, endometrial and colon cancer (3). By contrast, *PIK3CA* mutations are rare in highly aggressive metastatic prostate cancer. Instead, loss of PTEN due to loss of heterozygosity (LOH) or inactivating mutations is the predominant mechanism

Corresponding author: Alex Toker, Department of Pathology, Beth Israel Deaconess Medical Center, 330 Brookline Avenue, EC/CLS633A, Boston, MA, 02215, Tel: 617-735-2482, FAX: 617-735-2480, atoker@bidmc.harvard.edu.

Conflict of Interest Statement: No potential conflicts of interest to disclose.

driving PI 3-K pathway activation in prostate tumors (6, 7). The critical role of the PI 3-K pathway in tumorigenesis has led to the development of numerous small molecule inhibitors targeting PI 3-K (1). However, as a tumor suppressor PTEN has yet to be targeted therapeutically, and to this end downstream targets of PI 3-K and PTEN may provide more viable therapeutic strategies.

The best understood effector activated downstream of PI 3-K is the protein kinase Akt, which encompasses three isoforms, Akt1, Akt2 and Akt3 (8, 9). PIP_3 binds the Pleckstrin Homology domain of Akt effectively recruiting it to the plasma membrane, where it is activated by phosphorylation at Threonine 308 and Serine 473 by PDK1 and the mTOR Complex 2, respectively (10–12). Activated Akt then translocates to distinct subcellular compartments where it phosphorylates numerous substrates, many of which are oncogenes or tumor suppressors (13). The essential role of Akt in tumorigenesis has led to the development of a number of first-generation pan-Akt inhibitors currently in clinical trials (14). Although the three Akt isoforms share high degree of sequence identity and are regulated by similar mechanisms, studies have highlighted distinct functions of Akt isoforms in cancer progression (reviewed in (15)). For example whereas Akt2 promotes breast cancer cell migration and metastatic dissemination, Akt1 can actually function as a metastasis suppressor (9, 16–19). These and other studies suggest that Akt isoform-selective inhibitors might provide more optimal therapeutic responses in tumor-specific contexts.

A critical role for Akt in PTEN-deficient tumors is evident from a number of studies. PTEN heterozygous mice develop tumors spontaneously in multiple organs, concomitant with hyperphosphorylated Akt (20–22). Prostate tumor development induced by PTEN loss requires functional mTORC2 (23). Similarly, mice lacking Akt1 are protected from tumorigenesis induced by PTEN loss (24). Curiously, a more recent study indicated that inactivation of Akt2 has little or no consequence on prostate neoplasia, explained in part by the relatively little impact of Akt2 loss on total Akt activity and also an increase in blood insulin levels (25). By contrast, Akt2 is required for proliferation and invasive migration of PTEN-deficient glioblastoma (26, 27). In late-stage colorectal cancer, Akt2 is highly expressed and functions synergistically with PTEN loss to promote metastasis (28). It has also been demonstrated that deletion of Akt2 in PTEN-null mice attenuates hepatic injury, thereby delaying liver tumor development (29).

Although the contribution of Akt in tumor initiation in the context of PTEN inactivation has been determined, the role of Akt isoforms in the maintenance of established PTEN null tumors is unknown. Moreover, it is unclear whether PTEN-deficient tumors depend on specific Akt isoform(s) for survival signaling. Here we have used an inducible shRNA strategy to silence individual Akt isoforms in tumor spheroids grown in 3-dimensional (3D) culture. We find that in PTEN-deficient tumor cells depletion of Akt2 induces apoptosis and leads to regression of established prostate xenografts. By contrast, downregulation of Akt1 or Akt3 has no effect on the integrity of tumor spheroids. We also demonstrate that p21 is a downstream effector of Akt2 in modulating tumor cell survival. These data identify Akt2 as the critical isoform for driving maintenance of established PTEN-deficient cancers.

Results

Akt2 silencing induces prostate tumor spheroid disintegration

The role of Akt in the initiation of PTEN-deficient prostate tumors has been studied (24, 25). However, the function of Akt isoforms in modulating cancer cell survival in this context has not been determined. To assess the roles of Akt isoforms in tumor initiation as well as maintenance, we generated isoform-specific shRNAs in a doxycycline (dox)-regulated system. Due to the high frequency of PTEN inactivation (up to 50%) observed in human prostate cancers (6), we first introduced shRNAs in the PTEN-deficient prostate LNCaP line. Addition of dox to LNCaP cells results in highly selective silencing of Akt1 and Akt2 (LNCaP cells do not express Akt3; Fig. 1A). We next performed 3D spheroid assays with Matrigel, since growth of tumor cells in 3D more accurately recapitulates the morphology of tumors growing *in vivo*. Spheroid growth of cells containing control shRNA in the presence of with dox is indistinguishable from spheroids in the absence of dox. Conversely, depletion of Akt1 or Akt2 in LNCaP cells from the start of the assay results in compete inhibition of spheroid formation (Fig. 1B). Therefore, both Akt1 and Akt2 are required for initial tumor cell growth in 3D.

We next determined the contribution of Akt1 and Akt2 to tumor maintenance by allowing LNCaP spheroids to form for 7–13 days before dox treatment. Strikingly, Akt1 depletion has no effect on the maintenance of tumor spheroids in this assay. By contrast, silencing of Akt2 results in a complete disintegration of spheroids at 10 days post-dox treatment, with a noticeable change in morphology as early as 4 days post-dox (Fig. 1C).

Akt2, but not Akt1, regulates survival of PTEN-deficient prostate tumor cells

To determine if Akt2 depletion induces spheroid disintegration by promoting apoptosis, we stained spheroids for active caspase-3 followed by analysis with confocal microscopy. Akt1 silencing has no effect on the levels of active caspase-3, despite a dramatic down-regulation of Akt1 in tumor spheroids (Fig. 2A). By contrast, there is a robust induction of active caspase-3 upon Akt2 depletion (Fig. 2B). In addition, condensed apoptotic nuclei and marked disruption of cell morphology are observed in Akt2, but not Akt1, -depleted spheroids. Whereas a minimal number of apoptotic cells are observed in Akt1-silenced spheroids, more than 50% of cells in Akt2-depleted spheroids display active caspase-3 and fragmented nuclei (Fig. 2C).

To avoid potential shRNA off-target effects, we used a cDNA-rescue strategy. shRNA-resistant dox-inducible Akt1 and Akt2 sequences were generated and reintroduced into Akt2-depleted LNCaP cells. Apoptosis was assessed by staining cells with the apoptotic marker annexin V followed by FACS analysis. Whereas expression of Akt2 completely rescues apoptosis induced by Akt2 silencing, expression of Akt1 does not (Fig. 2D). In addition, robust apoptosis is induced when Akt2 is knocked down by an independent shRNA targeting a distinct region of the Akt2 transcript (Fig. 2E). The exclusive function of Akt2 in regulating survival in 3D was also observed in a distinct PTEN-null prostate line, PC3 (Fig. 2F). We also evaluated the activity of Akt small molecule inhibitors in PTEN-deficient prostate cancer survival. As expected, treatment of LNCaP spheroids with an Akt2-selective

inhibitor (EMD Millipore; IC_{50} = 0.8 μM for Akt2) inhibits spheroid growth in a dose-dependent manner (Fig. 2G). These data demonstrate that Akt2, but not Akt1, plays a critical and exclusive role in the maintenance of PTEN-deficient prostate cancer spheroids.

We next evaluated the consequence of Akt isoform depletion in conventional 2D culture. Silencing Akt1 or Akt2 significantly inhibits LNCaP cell proliferation to a similar extent (Fig. S1A), consistent with the essential role of Akt1 and Akt2 in proliferation that is observed in 3D. Silencing of Akt1 or Akt2 also suppresses cell migration in Transwell migration assays (Fig. S1B), indicating that both Akt1 and Akt2 are pro-migratory in LNCaP cells. However, depletion of Akt2 in cells grown in 2D does not induce apoptosis after 5 days of dox treatment, whereas the same cells grown as 3D spheroids undergo robust apoptosis upon Akt2 silencing (Fig. 3A). When cells in 2D culture were allowed to grow longer, apoptosis is observed after 7 days of dox treatment, although the effect is much more modest compared to Akt2-depleted 3D spheroids (Fig. 3B). We then addressed whether Akt1 or Akt2 depletion acts synergistically with chemotherapeutic agents to induce apoptosis in tumor cells in 2D culture. Apoptosis was assessed 3 days after dox treatment, when Akt1 or Akt2 knockdown alone has minimal effect on cell death (Fig. 3C). Depletion of Akt1 or Akt2 functions synergistically with doxorubicin to induce apoptosis of LNCaP cells. Taken together, these findings further demonstrate that Akt2 is both necessary and sufficient to regulate survival of PTEN-deficient prostate cancer cells in a manner that is robustly observed in 3D, but not 2D, culture.

PTEN-deficient tumor spheroids depend on Akt2 for survival

Since both LNCaP and PC3 cells are PTEN-deficient, we next investigated if Akt2 has an exclusive function in survival phenotypes in other solid tumors with high frequencies of PTEN inactivation, including glioblastoma and breast carcinoma. Similar to what is observed in prostate cancer cells, silencing of Akt1, Akt2 or Akt3 in PTEN-deficient MDA-MB-468 breast cancer cells attenuates proliferation in monolayer culture as well as inhibition of spheroid growth in 3D (Fig. S2A–B). However when MDA-MB-468 spheroids were allowed to form prior to dox administration, silencing of Akt2, but not Akt1 or Akt3, leads to spheroid disintegration and caspase-3 activation (Fig. 4A and 4B). Similar results are observed for a distinct PTEN-deficient breast cancer line, BT-549 (Fig. 4C). PTEN-deficient U87-MG glioblastoma cells form highly invasive spheroids in 3D culture. Whereas knockdown of Akt1 or Akt3 has no effect on spheroid phenotypes, Akt2 depletion results in regression of invasive spheroids and robust cell death (Fig. 4D). Furthermore, six other cancer lines that express wild-type PTEN (T47D, MCF10DCIS, SKBR3, H1703, SKOV3, and DU145) were analyzed and the data show that Akt1 or Akt2 silencing in these lines has no effect on spheroid integrity (Fig. S3A–G).

To more directly test the specific anti-apoptotic function of Akt2 in PTEN-deficient tumor spheroids, we used a molecular genetic approach in the prostate cell line CWr22-RV-1 that are PTEN wild-type. Upon knockdown of Akt1 or Akt2, robust spheroid disintegration is observed (Fig. 4E). Conversely, Akt3 silencing has no effect on spheroid growth or phenotypes. Strikingly, whereas disintegration is observed in Akt2-depleted spheroids regardless of PTEN expression or silencing, knockdown of PTEN completely rescues

spheroid disintegration mediated by Akt1 silencing (Fig. 4F). Collectively, these data indicate that PTEN-deficient tumor spheroids are addicted to Akt2 for survival signaling and maintenance, at least *in vitro*.

Identification of Akt2-specific targets: Role of p21 in Akt2-mediated spheroid maintenance

We next determined the molecular mechanisms that account for the exclusive function of Akt2 in tumor spheroid maintenance. Quantitative RT-PCR analysis shows that the expression levels of Akt1 and Akt2 in LNCaP cells are comparable (Fig. S4A). To examine the activation status of Akt1 and Akt2 in 3D cultures, we tested the effect of Akt isoform knockdown on the phosphorylation of total Akt as well as classical downstream pan-Akt substrates. Akt1 and Akt2 depletion results in a 70 and 20% reduction of pAkt Ser473, respectively (Fig. S4B). Interestingly, Akt1 plays a predominant role in the phosphorylation of GSK3β in LNCaP cells. Conversely, Akt2 knockdown has a more profound effect on the phosphorylation of PRAS40 compared to Akt1 knockdown. Taken together, these results suggest that both Akt1 and Akt2 are active in cells growing in 3D, and that the exclusive function of Akt2 cannot be accounted for by gross differences between the expression and activation status of individual Akt isoforms. To explore isoform-specific signaling, we used quantitative RT-PCR to assess the expression levels of pro-apoptotic proteins. Silencing of Akt1 or Akt2 in LNCaP spheroids growing in 3D results in upregulation of p53 and Puma message levels (Fig 5A). Surprisingly, whereas the mRNA levels of two targets of p53, p21 and Bax, are not affected by Akt1 depletion, knockdown of Akt2 significantly enhances p21 and Bax message. Immunoblot analysis shows that Akt2 silencing also leads to increased p21 and Bax protein expression when cells are cultured in both 2D and 3D (Fig. 5B). Upregulation of p21 and Bax by Akt2 silencing is also observed in two distinct PTEN-deficient lines, PC3 and U87-MG (Fig. 5C). Interestingly, reduced p21 protein levels are observed in Akt1-depleted LNCaP and PC3 cells, suggesting a general function for the Akt pathway in regulating the stability of p21, at least in prostate cancer (Fig. 5C).

To explore this further and evaluate if p21 is a downstream target of Akt2 in tumor maintenance, we used p21 shRNA in rescue experiments. Since it is established that p21 can modulate Akt-mediated cell cycle progression, we first assessed the effect of p21 knockdown on the cell cycle profile of Akt2-depleted cells. As expected, silencing of Akt2 leads to cell cycle arrest, and silencing of p21 restores cell cycle progression in Akt2-depleted cells (Fig. S5). We then evaluated the contribution of p21 in Akt2-mediated spheroid maintenance. Whereas knockdown of p21 alone has no effect on cell death, apoptosis mediated by Akt2 depletion is quantitatively rescued by p21 silencing (Fig. 5D), indicating that p21 is at least one downstream target of Akt2 that regulates apoptotic response. We have also examined if the pro-apoptotic protein Bax is a mediator of Akt2 in regulating prostate spheroid maintenance. Knockdown of Bax results in a small but statistically significant reduction in apoptosis (Fig. S6). However, Bax depletion does not rescue apoptosis induced by Akt2 knockdown, suggesting that Bax does not play a role in Akt2-mediated spheroid maintenance.

Inhibition of Akt results in the relief of negative feedback pro-survival pathways which in turn lead to upregulation of growth factor receptor tyrosine kinases (30). Consistent with this

model, treatment of LNCaP spheroids with the pan-Akt inhibitor GSK690693 reduces phosphorylation of the Akt substrate PRAS40, yet leads to increased IGF-1Rβ expression (Fig. 5E). Conversely, the levels of p21 do not change with pan-Akt inhibitor treatment, consistent with the opposing effects of Akt1 and Akt2 on p21 expression. Moreover, silencing of Akt1 in 2D as well as 3D leads to elevated IGF-1R mRNA, but this does not translate into changes in IGF-1R total protein (Fig. 5B and 5F). Conversely, Akt2 depletion in 3D, but not 2D, dramatically reduces IGF-1R protein as well as mRNA levels (Fig. 5B and 5F). Inhibition of IGF1R with NVP AEW541 does not induce apoptosis in LNCaP tumor spheroids (Fig. 5G). Interestingly, whereas concomitant inhibition of IGF1R and Akt1 depletion has no effect on spheroid maintenance, NVP AEW541 acts synergistically with Akt2 knockdown in potentiating apoptosis. The concomitant induction of pro-apoptotic proteins and decrease of pro-survival proteins in tumor spheroids by Akt2 depletion may explain the more robust apoptotic phenotype observed in in 3D cultures when compared to 2D.

Akt2 depletion induces prostate tumor regression in a xenograft model

Finally, using inducible Akt isoform shRNA we investigated the relative contribution of Akt1 and Akt2 in the maintenance of established tumors *in vivo*. LNCaP cells harboring dox-inducible Akt1 or Akt2 shRNA were injected subcutaneously into nude mice. Once tumors reached a critical palpable mass, dox was administered for 12 days to induce shRNA expression. In the absence of dox, tumors containing Akt1 or Akt2 shRNA double in relative size (Fig. 6A, S7). Akt1 silencing robustly reduces tumor growth (+39% vs. +116%; +dox vs. −dox; $P < 0.05$), indicative of the expected cytostatic effect given the essential role of Akt1 in cell proliferation (see Fig. 1B). In striking contrast, tumors regress significantly upon Akt2 silencing (−49% vs. +93%; +dox vs. −dox; $P < 0.001$). To confirm knockdown of Akt1 and Akt2 and assess their effects on apoptosis, tumors were harvested at the end of the study. Both isoforms are significantly silenced by their respective shRNA's (Fig 6B). Consistent with our cell-based analyses, active caspase-3 levels are increased in Akt2-depleted xenografts but not in Akt1-depleted tumors. Moreover, similar to that observed in *in vitro* tumor spheroids, depletion of Akt2, but not Akt1, significantly induces p21 expression (Fig. 6B). Taken together, these data demonstrate that prostate tumors deficient in PTEN are exclusively addicted to Akt2 for tumor maintenance, and that inhibiting Akt2 signaling induced tumor regression.

Discussion

PTEN inactivation is a common event in prostate cancer with frequencies ranging from 30 to 60%, and is associated with aggressive tumor progression and poor prognosis (31). However, to date PTEN has proven to be an intractable target for drug development due to the therapeutic challenges associated with reactivation of a tumor suppressor. Although numerous studies have established the functional importance of Akt activation in PTEN-deficient tumors, the specific contributions of Akt isoforms in mediating the proliferative and survival signals necessary for tumor initiation and maintenance have not been explored. The present work expands on previous studies that have concluded that both Akt1 and Akt2 function to modulate prostate cancer cell proliferation (32). However, our studies point to a

critical and exclusive function for Akt2 in mediating the signals necessary for PTEN-deficient tumor cell maintenance and survival. One important aspect that previously had not been considered is the assessment of survival in 3D spheroids, whereby induction of apoptosis is observed only upon Akt2, but not Akt1 or Akt3 silencing. The function of Akt2 in PTEN-driven tumor maintenance is also corroborated by depletion of PTEN in PTEN wild-type prostate cancer cells, which is sufficient to render them exclusively Akt2-dependent. Importantly, the addiction of PTEN-deficient tumors to Akt2 signaling is observed not only in prostate cancer, but also in PTEN-null breast and glioblastoma spheroids. Of particular clinical importance, we also find that both breast, prostate, lung and ovarian tumor lines that express wild type PTEN, but display hyperactive Akt signaling due to other pathway lesions such as oncogenic *PIK3CA* or receptor amplification, do not depend exclusively on Akt2 activity for survival. These findings advocate for the development of Akt2-selective inhibitors and also suggest that PTEN deficiency could be used as a patient tailoring strategy for therapeutic benefit.

Several potential mechanisms may contribute to the addiction of Akt2 in *PTEN*-deficient but not in *PIK3CA* mutant tumor cells. It is well-established that PTEN antagonizes PI 3-K/Akt pathway by acting as a PIP3 phosphatase. More recent studies have shown that nuclear PTEN functions as an essential tumor suppressor, and regulates chromosome stability as well as cell cycle arrest (33, 34). It is possible that nuclear PTEN specifically antagonizes Akt2 activity in the nucleus, such that PTEN inactivation results in the accumulation of hyperactive nuclear Akt2 and affords a dominant effect of Akt2 on tumor maintenance. It has also been shown that in certain tumor contexts, p110β but not p110α plays a critical role in *PTEN*-deficient prostate tumorigenesis (7, 35). It would be interesting to examine if p110β cooperates with Akt2 to mediate survival signaling in *PTEN*-null tumor spheroids.

Previous studies have shown that Akt1 depletion markedly reduces the incidence of prostate tumors in PTEN heterozygous mice (24), whereas Akt2 depletion has little or no effect (25). These results suggest that Akt1, but not Akt2, plays an critical role in prostate tumor initiation. By contrast, our studies demonstrate that Akt2, but not Akt1, is necessary for tumor maintenance and survival, since Akt2 depletion alone induces regression of prostate xenografts. This finding has significant clinical implications, since studies have shown that inhibition of a number of oncogenic proteins in the PI 3-K pathway, including p110α and mTOR, only have cytostatic effects in xenograft models (36, 37). However, regression of established tumors is not commonly observed, possibly due to the relief of feedback suppression mechanisms. In this context, inhibition of Akt relieves feedback suppression by inducing the expression of multiple receptor tyrosine kinases (30). This is consistent with our finding that inhibiting Akt activity in prostate cancer cells induces expression of IGF-1R. Interestingly, silencing Akt2, but not Akt1, leads to reduced IGF-1R expression in tumor spheroids. These data further point to an unmet need for the development of Akt2-selective inhibitors for PTEN-null tumors.

A separate line of evidence in support for the development of Akt isoform-selective inhibitors comes from findings of the control of tumor invasion and metastasis that are differentially regulated by Akt1 and Akt2 (9). Considering other potential isoform-specific functions of Akt such as metabolism and stem cell maintenance, one prediction is that

isoform-selective inhibitors would offer less toxicity and other unwanted on-target effects. Indeed, PI 3-K isoform-specific inhibitors (e.g. CAL-101 for PI3Kδ) offer clear-cut examples of powerful single agents in treating selected cancer types and patient populations (38).

The potent regression of prostate xenografts achieved by Akt2 inhibition is accompanied by a robust induction of p21. Using cDNA rescue experiments, we show that p21 is one critical downstream effector of Akt2 in the apoptotic response, and as such could serve as a potential biomarker used for screening Akt2 activity *in vivo*. In addition to its classical role as a cyclin-dependent kinase inhibitor, p21 has been shown to act as a pro-apoptotic or anti-apoptotic protein, depending on the tumor context as well as intracellular localization (39). Overexpression of p21 in glioma and ovarian cancer cells enhances apoptosis induced by chemotherapeutic agents (40, 41). Moreover, adenoviral gene transfer of p21 induces apoptosis in established cervical xenografts (42). Similarly, a chimeric peptide comprising the carboxyl terminus of p21 conjugated to a pentapeptide induces apoptosis in lymphoma cells (39). The mechanism by which p21 induces apoptosis has not been well studied. In hepatoma cells p21 expression promotes ceramide-induced apoptosis through the proapoptotic protein Bax (43). Our analysis also reveals a concomitant induction of p21 and Bax in a variety of Akt2-depleted PTEN-deficient cancer cell lines. However, rescue experiments indicate that Bax does not play an essential role in Akt2-mediated tumor maintenance.

We further show that Akt2 regulates p21 at the mRNA level. However the precise mechanism is not known. p21 is a direct target of p53 (44), however we have been unable to detect a robust alterations of p53 activity upon Akt2 inhibition or silencing. Moreover, p21 expression is also regulated by a variety of other transcription factors including Ap2, STATs, C/EBPs and MyoD (45). Interestingly, Akt2 has a distinct function in modulating the transactivation activity of MyoD-MEF2 (46). Whether Akt2 modulates p21 expression via MyoD in PTEN-deficient cells remains to be determined.

One important concept that has emerged from our studies is the profound difference observed in the ability of Akt2 and Akt1 to mediate survival and maintenance of PTEN-deficient tumor cells in 3D culture versus growth on 2 dimensions. The altered molecular behavior of cells in 3D compared with growth in 2D has been reported by many groups and so it has been proposed that growth in 3D serves as a better model for the responsiveness of tumors to therapy in patients. For example, in triple-negative breast cancer, increased sensitivity to MEK inhibitors is observed in 3D cultures when compared to monolayer models (47). It has also been shown that in Her2-overexpressing breast cancers, cells grown in 3D have enhanced activation of Her2 as compared to growth in 2D, resulting in an increased response to trastuzumab (48). One report indicates that mitochondrial DNA depletion in prostate epithelial cells enhances PI 3-K/Akt2 activation which in turn promotes anoikis resistance (49). We therefore examined if the response of tumor cells to Akt2 silencing could be due to the enhanced activation of this isoform when cells are grown in 3D. However, our data show that that the differential effects on apoptosis cannot be explained by differences in Akt2 activation levels compared to Akt1, at least when Akt1 and Akt2 phosphorylation and activity are analyzed in whole cell lysates. One possibility is that

a distinct intracellular localization of Akt2, especially evident when cells are grown in 3D culture, offers the appropriate platform for protein-protein interactions and accessibility to specific Akt2 substrates and targets, such as p21, that in turn mediate the survival response in PTEN-deficient tumor cells. In this model, Akt1 localization would not phenocopy Akt2 in the survival response, nor would growth in 2D monolayer culture. Whether this models accounts for the exclusive function of Akt2 in mediating tumor maintenance of PTEN-deficient tumors remains to be determined.

Taken together, our findings demonstrate that Akt2 and its downstream targets are responsible for driving PTEN-null tumor progression, and identify Akt2 as an important target for the effective treatment of PTEN-deficient solid tumors. They also further advocate for the development of Akt isoform-specific inhibitors, analogous to the selective PI 3-kinase p110 isoform selective inhibitors currently in pre-clinical development.

Materials and Methods

Cell Culture

MDA-MB-468, U87-MG and HEK293T cells were obtained from ATCC and maintained in Dulbecco's modified Eagle medium (DMEM; Cellgro) supplemented with 10% tet system-approved Fetal Bovine Serum (FBS; Clontech). LNCaP, PC3, BT-549 and CWr2-RV-1 cells were cultured in RPMI 1640 medium (Cambrex) supplemented with 10% FBS. All cell lines obtained from the cell banks listed above are tested for authentication using STR (short tandem repeat) profiling and passaged for fewer than 6 months, and routinely assayed for mycoplasma contamination.

3D cultures

3D cultures were prepared as previously described (50). Briefly, chamber slides were coated with growth factor-reduced Matrigel (BD Biosciences) and allowed to solidify for 30 min. 2,000 – 4,000 cells in assay medium were seeded on coated chamber slides. Assay medium contained DMEM or RPMI 1640 supplemented with 10% FBS and 2% Matrigel. Assay medium for U87-MG cells contained RPMI 1640 medium supplemented with 2% FBS and 5% Matrigel. The assay medium was replaced every 4 days. 100 ng ml^{-1} doxycycline (dox) was added every 2 or 3 days. For Annexin V apoptosis assays and Western blot analysis, 3D cultures were set up in Ultra-low adherent 6-well plates (Corning). Cells were seeded in 1.5 ml assay medium contained DMEM or RPMI 1640 supplemented with 10% FBS and 2% Matrigel. 1.5 ml assay medium was added every 4 days. Morphology of spheroids grown in ultra-low adherent plates is similar to those grown in Matrigel coated on chamber slides.

Antibodies

Anti-Akt1, anti-Akt2, anti-Akt3, anti-phospho-Akt S473 (pAkt), anti-phospho-Akt1 S473 (pAkt1), anti-phospho-Akt2 S474 (pAkt2), anti-Bax, anti-p53, anti-PUMA, anti-IGF1Rβ, anti-pGSK3β, anti-GSK3β, anti-p21, anti-PRAS40, anti-pPRAS40, anti-HA and anti-active caspase 3 antibodies were obtained from Cell Signaling Technology. Anti-β-actin antibody was purchased from Sigma-Aldrich. Anti-p85 polyclonal antibody was generated in-house

and has been described (51). Horseradish peroxidase-conjugated anti-mouse and anti-rabbit immunoglobulin G (IgG) antibody were purchased from Chemicon.

RNA interference

For dox-inducible shRNA-mediated knockdown of Akt isoforms, a set of single-stranded oligonucleotides encoding the Akt1, Akt2 and Akt3 target shRNA and its complement were synthesized. The hairpin sequences have been validated (17). Akt1, sense, 5′-CCGGGAGTTTGAGTACCTGAAGCTGCTCGAGCAGCTTCAGGTACTCAAACTCTTTTTG–3′; Akt2, sense, 5′–CCGGGCGTGGTGAATACATCAAGACCTCGAGGTCTTGATGTATTCACCACGCTTTTTG–3′; Akt3, sense, 5′–CCGGCTGCCTTGGACTATCTACATTCTCGAGAATGTAGATAGTCCAAGGCAGTTTTTG–3′. Akt2 #2, sense, 5′–CCGGCTTCGACTATCTCAAACTCCTCTCGAGAGGAGTTTGAGATAGTCGAAGTTTTTG–3′. The oligonucleotide sense and antisense pair were annealed and inserted into tet-on pLKO. To produce lentiviral supernatants, 293T cells were co-transfected with control or shRNA-containing tet-on pLKO vectors, VSVG and psPAX2 for 48 h. p21 and Bax shRNA sequences (p21 sense, 5′–CCGGGACAGCAGAGGAAGACCATGTCTCGAGACATGGTCTTCCTCTGCTGTCTTTTTG–3′. Bax sense, 5′–CCGGAAGGTGCCGGAACTGATCAGACTCGAGTCTGATCAGTTCCGGCACCTTTTTTTG–3′) has been validated (52, 53) and was cloned into the tet-on pLKO lentiviral expression system as described above. Cells stably expressing dox-inducible shRNA were cultured in medium containing puromycin (0.5–2 μg ml^{-1}). Gene knockdown was induced by incubating cells with 100 ng ml^{-1} dox for 48 to 72 h.

Plasmids

For dox-inducible over-expression of Akt1 and Akt2, HA-Akt1/pTRIPZ and HA-Akt2/pTRIPZ were constructed. HA-Akt1 and HA-Akt2 cDNAs were amplified by PCR from HA-Akt1/pcDNA3 and HA-Akt2/pcDNA3, respectively. The resulting PCR product was digested with restriction enzymes AgeI and ClaI, followed by insertion into pTRIPZ lentiviral vector (Thermo Scientific). shRNA-resistant variants of Akt were constructed by site-directed mutagenesis with the following primers: Akt1 Sense, 5′–GCACCGCGTGACCATGAACGAGTTCGAATATCTCAAGCTGCTGGGCA–3′; Akt2 Sense, 5′–CTGGCTCCACAAGCGTGGAGAGTATATTAAGACCTGGAGGCCACGG–3′. All sequences were verified by DNA sequencing.

Immunofluorescence and confocal analysis

Tumor spheroids embedded in Matrigel in chamber slides were fixed with 4% paraformaldehyde for 20 min and permeabilized with 0.5% Triton X-100 for 2 min. Cells were rinsed with glycine/PBS (130 mM NaCl; 7 mM Na_2HPO_4; 3.5 mM NaH_2PO_4; 100 mM glycine) three times. Cells were then blocked with 10% goat serum and 20 μg ml^{-1} of goat anti-mouse $F(ab')_2$ in IF Buffer (130 mM NaCl; 7 mM Na_2HPO_4; 3.5 mM NaH_2PO4; 7.7 mM NaN_3; 0.1% BSA; 0.2% Triton X-100; 0.05% Tween-20) for 45 min and incubated with primary antibody for 2 h. After washing three times with IF buffer, cells were

incubated with Cy3-conjugated anti-rabbit IgG antibody for 45 min. F-actin was visualized with Alexa Fluor 488-conjugated phalloidin or Alexa Fluor 647-conjugated phalloidin (Invitrogen). Cells were then rinsed once with IF buffer and twice with PBS and then mounted with Prolong Gold antifade reagent/4,6-diamidino-2-phenylindole (DAPI) (Pierce). Confocal images of cells were acquired using a confocal microscope and digital image analysis software (LSM 510 Meta; Zeiss).

Annexin V apoptosis assay

3D spheroids grown in ultra-low adherent plates were collected by centrifugation at 800x g for 5 min. Cells in spheroids were trypsinized at 37°C for 3 min, followed by staining with annexin V and 7-AAD with PE Annexin V apoptosis detection kit (BD Pharmingen). Briefly, cells were washed twice with PBS and stained with 5 μl of PE-annexin V and 5 μl 7-AAD in binding buffer for 15 min. FACS analysis was performed with FACSCalibur (Becton-Dickinson) and FlowJo (Tree Star Inc) software.

Cell cycle analysis

Cells were washed with PBS twice at 4°C, and then fixed with 70% ethanol at −20°C for 2 h. After washing once with PBS, cells were incubated with 1 μg/ml RNase and 50 μg/ml PI (Roche) for 37°C for 30 min, followed by incubation at 4°C for 1 h in the dark. FACS analysis was performed with FACSCalibur (Becton-Dickinson) and FlowJo (Tree Star Inc) software.

Xenograft studies

Male nude mice (5–6 weeks old) were purchased from Taconic and maintained and treated under specific pathogen-free conditions. All procedures were approved by the Institutional Animal Care and Use Committee at Beth Israel Deaconess Medical Center and conform to the federal guidelines for the care and maintenance of laboratory animals. The mice were injected subcutaneously with 9×10^6 LNCaP cells in media with 50% Matrigel. Tumor formation was examined every 2 to 3 days for the duration of the experiment. Mice with palpable tumors were randomly divided into control and treatment groups and treated with water supplemented with 1 mg ml^{-1} dox and 2% sucrose, or standard water supply for 12 days. Bottles of water/dox were changed twice a week. Tumor volume was measured on the first day of dox treatment, as well as day 12 post-dox treatment. Tumor volume = $(4/3)(\pi)$ (R1 × R2 × R3); R = radius. Tumors were harvested at the experimental endpoint.

Immunohistochemistry of FFPE xenograft tumors

Xenograft tumors were deparaffinized in xylene and hydrated in a series of ethanol washes. After heat-induced antigen retrieval in citrate buffer (pH 6), the samples were blocked with donkey serum. Slides were then incubated with primary antibodies for overnight at 4°C. Samples were washed three times with TBS followed by incubation with biotinylated secondary antibodies for one hour. The slides were washed and developed using the Diaminobenzidine (DAB) metal enhanced kit (Vector lab) and counter-stained with hematoxylin.

Transwell migration assays

1×10^5 cells in serum-free medium containing 0.1% BSA were added to upper Transwell chambers in triplicate. NIH 3T3-cell-conditioned medium was added to the lower chambers. After 2–16 h incubation at 37°C, non-migrated cells on Transwell filters (8 μm pore size; Corning) were removed. Cells that had migrated to the bottom of the filters were fixed and stained using the Hema-3 stain set (Protocol).

Quantitative real-time-PCR

Total RNA was isolated with RNeasy Mini Kit (Qiagen) according to manufacturer's protocol. Reverse transcription was performed using random hexamers and multiscribe reverse transcriptase (Applied Biosystems, Foster City, CA). Quantitative real-time PCR was performed using an ABI Prism 7700 sequence detector (Foster City, CA). Akt1 primer: sense, 5′–CAAGCCCAAGCACCGC–3′, anti-sense, 5′–GGATCACCTTGCCGAAAGTG–3′ (54); Akt2 primer: sense, 5′–GCAAGGCACGGGCTAAAG–3′, anti-sense, 5′–CCCGCACCAGGATGACTT–3′ (54); p21 primer: sense, 5′–CGCGACTGTGATGCGCTAATG–3′, anti-sense, 5′–GGAACCTCTCATTCAACCGCC–3′ (55); p53 primer: sense, 5′–TGCAGCTGTGGGTTGATTC–3′, anti-sense, 5′–TCCGTCCCAGTAGATTACCA–3′ (55); IGF1R primer: sense, 5′–TTCAGCGCTGCTGATGTG–3′, anti-sense, 5′–GGCTCATGGTGATCTTCTCC–3′ (56); Puma primer: sense, 5′–GACGACCTCAACGCACAGTA–3′, anti-sense, 5′–AGGAGTCCCATGATGAGATTGT–3′ (57); Bax primer: sense, 5′-TGG AGCTGCAGAGGATGATTG-3′, anti-sense, 5′–GAAGTTGCCGTCAGAAAACATG–3′ (58). PCR reactions were carried out in triplicate. Quantification of mRNA expression was calculated by the dCT method with GAPDH as the reference gene.

Immunoblotting

Cells were washed with PBS at 4°C and lysed in EBC buffer (0.5% NP-40, 120 mM NaCl, 50 mM Tris-HCl (pH 7.4), proteinase inhibitor cocktail, 50 nM calyculin, 1 mM sodium pyrophosphate, 20 mM sodium fluoride, 2 mM EDTA, 2 mM EGTA) for 25 min on ice. Cell extracts were pre-cleared by centrifugation at 13,000 rpm for 10 min at 4°C and protein concentration was measured with the Bio-Rad protein assay reagent using a Beckman Coulter DU-800 machine. Lysates were then resolved on 8% acrylamide gels by SDS-PAGE and transferred electrophoretically to nitrocellulose membrane (BioRad) at 160 mA for 80 min. The blots were blocked in TBST buffer (10 mM Tris-HCl, pH 8, 150 mM NaCl, 0.2% Tween 20) containing 5% (w/v) nonfat dry milk for 30 min, and then incubated with the specific primary antibody diluted in blocking buffer at 4°C overnight. Membranes were washed three times in TBST, and incubated with horseradish peroxidase-conjugated secondary antibody for 1 h at room temperature. Membranes were washed 3 times and developed using enhanced chemiluminescence substrate (Pierce). Protein levels were quantified with ImageJ software.

Statistical analysis

Statistical significance between conditions was assessed by Student's *t* tests. In all figures, data are presented as mean ± standard error of the mean (SEM) for one representative

experiment. Significance between conditions is denoted as $*P < 0.05$, $**P < 0.01$, and $***P < 0.001$. For Transwell migration analyses, at least 5 random images were counted and averaged per well, for three wells, for each condition. At least three independent experiments were performed for each condition for verification of the emphasized trends in *in vitro* studies. For xenograft studies, at least seven tumors in each condition were analyzed.

Supplementary Material

Refer to Web version on PubMed Central for supplementary material.

Acknowledgments

We thank Casey Stottrup for technical assistance; the confocal imaging core and histology core at BIDMC for their technical support with immunohistochemistry; Sen Chen and the animal facility at BIDMC for their technical support with xenograft studies; and members of the Toker laboratory for discussions. This study was supported in part by grants from the National Institutes of Health (R.C., K99CA157945; A.T., CA092644; T32 CA081156-09; S.B., P01 CA163227; X.Y., 1R01 DK079962), the Department of Defense (S.B., W81XWH-09-1-0435) and a sponsored research grant from ImClone/Eli Lilly Inc. (A.T and R.C.).

References

1. Engelman JA. Targeting PI3K signalling in cancer: opportunities, challenges and limitations. Nat Rev Cancer. 2009; 9:550–62. [PubMed: 19629070]
2. Cantley LC. The phosphoinositide 3-kinase pathway. Science. 2002; 296:1655–7. [PubMed: 12040186]
3. Vanhaesebroeck B, Waterfield MD. Signaling by distinct classes of phosphoinositide 3-kinases. Experimental cell research. 1999; 253:239–54. [PubMed: 10579926]
4. Li J, Yen C, Liaw D, Podsypanina K, Bose S, Wang SI, et al. PTEN, a putative protein tyrosine phosphatase gene mutated in human brain, breast, and prostate cancer [see comments]. Science. 1997; 275:1943–7. [PubMed: 9072974]
5. Maehama T, Dixon JE. The tumor suppressor, PTEN/MMAC1, dephosphorylates the lipid second messenger, phosphatidylinositol 3,4,5-trisphosphate. The Journal of biological chemistry. 1998; 273:13375–8. [PubMed: 9593664]
6. Cairns P, Okami K, Halachmi S, Halachmi N, Esteller M, Herman JG, et al. Frequent inactivation of PTEN/MMAC1 in primary prostate cancer. Cancer research. 1997; 57:4997–5000. [PubMed: 9371490]
7. Jiang X, Chen S, Asara JM, Balk SP. Phosphoinositide 3-kinase pathway activation in phosphate and tensin homolog (PTEN)-deficient prostate cancer cells is independent of receptor tyrosine kinases and mediated by the p110beta and p110delta catalytic subunits. The Journal of biological chemistry. 2010; 285:14980–9. [PubMed: 20231295]
8. Bellacosa A, Testa JR, Staal SP, Tsichlis PN. A retroviral oncogene, akt, encoding a serine-threonine kinase containing an SH2-like region. Science. 1991; 254:274–7. [PubMed: 1833819]
9. Chin YR, Toker A. Function of Akt/PKB signaling to cell motility, invasion and the tumor stroma in cancer. Cellular signalling. 2009; 21:470–6. [PubMed: 19110052]
10. Alessi DR, James SR, Downes CP, Holmes AB, Gaffney PR, Reese CB, et al. Characterization of a 3-phosphoinositide-dependent protein kinase which phosphorylates and activates protein kinase Balpha. Curr Biol. 1997; 7:261–9. [PubMed: 9094314]
11. Stokoe D, Stephens LR, Copeland T, Gaffney PR, Reese CB, Painter GF, et al. Dual role of phosphatidylinositol-3,4,5-trisphosphate in the activation of protein kinase B. Science. 1997; 277:567–70. [PubMed: 9228007]
12. Sarbassov DD, Guertin DA, Ali SM, Sabatini DM. Phosphorylation and regulation of Akt/PKB by the rictor-mTOR complex. Science. 2005; 307:1098–101. [PubMed: 15718470]

13. Manning BD, Cantley LC. AKT/PKB signaling: navigating downstream. Cell. 2007; 129:1261–74. [PubMed: 17604717]
14. Liu P, Cheng H, Roberts TM, Zhao JJ. Targeting the phosphoinositide 3-kinase pathway in cancer. Nat Rev Drug Discov. 2009; 8:627–44. [PubMed: 19644473]
15. Dillon RL, Muller WJ. Distinct biological roles for the akt family in mammary tumor progression. Cancer research. 2010; 70:4260–4. [PubMed: 20424120]
16. Hutchinson JN, Jin J, Cardiff RD, Woodgett JR, Muller WJ. Activation of Akt-1 (PKB-alpha) can accelerate ErbB-2-mediated mammary tumorigenesis but suppresses tumor invasion. Cancer research. 2004; 64:3171–8. [PubMed: 15126356]
17. Irie HY, Pearline RV, Grueneberg D, Hsia M, Ravichandran P, Kothari N, et al. Distinct roles of Akt1 and Akt2 in regulating cell migration and epithelial-mesenchymal transition. J Cell Biol. 2005; 171:1023–34. [PubMed: 16365168]
18. Yoeli-Lerner M, Yiu GK, Rabinovitz I, Erhardt P, Jauliac S, Toker A. Akt blocks breast cancer cell motility and invasion through the transcription factor NFAT. Molecular cell. 2005; 20:539–50. [PubMed: 16307918]
19. Arboleda MJ, Lyons JF, Kabbinavar FF, Bray MR, Snow BE, Ayala R, et al. Overexpression of AKT2/protein kinase Bbeta leads to up-regulation of beta1 integrins, increased invasion, and metastasis of human breast and ovarian cancer cells. Cancer research. 2003; 63:196–206. [PubMed: 12517798]
20. Di Cristofano A, Pesce B, Cordon-Cardo C, Pandolfi PP. Pten is essential for embryonic development and tumour suppression. Nat Genet. 1998; 19:348–55. [PubMed: 9697695]
21. Freeman D, Lesche R, Kertesz N, Wang S, Li G, Gao J, et al. Genetic background controls tumor development in PTEN-deficient mice. Cancer research. 2006; 66:6492–6. [PubMed: 16818619]
22. Suzuki A, de la Pompa JL, Stambolic V, Elia AJ, Sasaki T, del Barco Barrantes I, et al. High cancer susceptibility and embryonic lethality associated with mutation of the PTEN tumor suppressor gene in mice. Curr Biol. 1998; 8:1169–78. [PubMed: 9799734]
23. Guertin DA, Stevens DM, Saitoh M, Kinkel S, Crosby K, Sheen JH, et al. mTOR complex 2 is required for the development of prostate cancer induced by Pten loss in mice. Cancer cell. 2009; 15:148–59. [PubMed: 19185849]
24. Chen ML, Xu PZ, Peng XD, Chen WS, Guzman G, Yang X, et al. The deficiency of Akt1 is sufficient to suppress tumor development in Pten+/− mice. Genes & development. 2006; 20:1569–74. [PubMed: 16778075]
25. Xu PZ, Chen ML, Jeon SM, Peng XD, Hay N. The effect Akt2 deletion on tumor development in Pten(+/−) mice. Oncogene. 2012; 31:518–26. [PubMed: 21743498]
26. Zhang B, Gu F, She C, Guo H, Li W, Niu R, et al. Reduction of Akt2 inhibits migration and invasion of glioma cells. International journal of cancer Journal international du cancer. 2009; 125:585–95. [PubMed: 19330838]
27. Cui Y, Wang Q, Wang J, Dong Y, Luo C, Hu G, et al. Knockdown of AKT2 expression by RNA interference inhibits proliferation, enhances apoptosis, and increases chemosensitivity to the anticancer drug VM-26 in U87 glioma cells. Brain research. 2012; 1469:1–9. [PubMed: 22771706]
28. Rychahou PG, Kang J, Gulhati P, Doan HQ, Chen LA, Xiao SY, et al. Akt2 overexpression plays a critical role in the establishment of colorectal cancer metastasis. Proceedings of the National Academy of Sciences of the United States of America. 2008; 105:20315–20. [PubMed: 19075230]
29. Galicia VA, He L, Dang H, Kanel G, Vendryes C, French BA, et al. Expansion of hepatic tumor progenitor cells in Pten-null mice requires liver injury and is reversed by loss of AKT2. Gastroenterology. 2010; 139:2170–82. [PubMed: 20837017]
30. Chandarlapaty S, Sawai A, Scaltriti M, Rodrik-Outmezguine V, Grbovic-Huezo O, Serra V, et al. AKT inhibition relieves feedback suppression of receptor tyrosine kinase expression and activity. Cancer cell. 2011; 19:58–71. [PubMed: 21215704]
31. Yoshimoto M, Cunha IW, Coudry RA, Fonseca FP, Torres CH, Soares FA, et al. FISH analysis of 107 prostate cancers shows that PTEN genomic deletion is associated with poor clinical outcome. Br J Cancer. 2007; 97:678–85. [PubMed: 17700571]

32. Sasaki T, Nakashiro K, Tanaka H, Azuma K, Goda H, Hara S, et al. Knockdown of Akt isoforms by RNA silencing suppresses the growth of human prostate cancer cells in vitro and in vivo. Biochemical and biophysical research communications. 2010; 399:79–83. [PubMed: 20638364]
33. Trotman LC, Wang X, Alimonti A, Chen Z, Teruya-Feldstein J, Yang H, et al. Ubiquitination regulates PTEN nuclear import and tumor suppression. Cell. 2007; 128:141–56. [PubMed: 17218261]
34. Shen WH, Balajee AS, Wang J, Wu H, Eng C, Pandolfi PP, et al. Essential role for nuclear PTEN in maintaining chromosomal integrity. Cell. 2007; 128:157–70. [PubMed: 17218262]
35. Jia S, Liu Z, Zhang S, Liu P, Zhang L, Lee SH, et al. Essential roles of PI(3)K- p110beta in cell growth, metabolism and tumorigenesis. Nature. 2008; 454:776–9. [PubMed: 18594509]
36. Wee S, Wiederschain D, Maira SM, Loo A, Miller C, deBeaumont R, et al. PTEN- deficient cancers depend on PIK3CB. Proceedings of the National Academy of Sciences of the United States of America. 2008; 105:13057–62. [PubMed: 18755892]
37. Shoji K, Oda K, Kashiyama T, Ikeda Y, Nakagawa S, Sone K, et al. Genotype- dependent efficacy of a dual PI3K/mTOR inhibitor, NVP-BEZ235, and an mTOR inhibitor, RAD001, in endometrial carcinomas. PLoS One. 2012; 7:e37431. [PubMed: 22662154]
38. Fruman DA, Rommel C. PI3Kdelta inhibitors in cancer: rationale and serendipity merge in the clinic. Cancer discovery. 2011; 1:562–72. [PubMed: 22586681]
39. Dong C, Li Q, Lyu SC, Krensky AM, Clayberger C. A novel apoptosis pathway activated by the carboxyl terminus of p21. Blood. 2005; 105:1187–94. [PubMed: 15466931]
40. Kondo S, Barna BP, Kondo Y, Tanaka Y, Casey G, Liu J, et al. WAF1/CIP1 increases the susceptibility of p53 non-functional malignant glioma cells to cisplatin- induced apoptosis. Oncogene. 1996; 13:1279–85. [PubMed: 8808702]
41. Lincet H, Poulain L, Remy JS, Deslandes E, Duigou F, Gauduchon P, et al. The p21(cip1/waf1) cyclin-dependent kinase inhibitor enhances the cytotoxic effect of cisplatin in human ovarian carcinoma cells. Cancer Lett. 2000; 161:17–26. [PubMed: 11078909]
42. Tsao YP, Huang SJ, Chang JL, Hsieh JT, Pong RC, Chen SL. Adenovirus- mediated p21((WAF1/SDII/CIP1)) gene transfer induces apoptosis of human cervical cancer cell lines. Journal of virology. 1999; 73:4983–90. [PubMed: 10233960]
43. Kang KH, Kim WH, Choi KH. p21 promotes ceramide-induced apoptosis and antagonizes the antideath effect of Bcl-2 in human hepatocarcinoma cells. Experimental cell research. 1999; 253:403–12. [PubMed: 10585263]
44. Levine AJ. p53, the cellular gatekeeper for growth and division. Cell. 1997; 88:323–31. [PubMed: 9039259]
45. Gartel AL, Tyner AL. The role of the cyclin-dependent kinase inhibitor p21 in apoptosis. Mol Cancer Ther. 2002; 1:639–49. [PubMed: 12479224]
46. Kaneko S, Feldman RI, Yu L, Wu Z, Gritsko T, Shelley SA, et al. Positive feedback regulation between Akt2 and MyoD during muscle differentiation. Cloning of Akt2 promoter. The Journal of biological chemistry. 2002; 277:23230–5. [PubMed: 11948187]
47. Li Q, Chow AB, Mattingly RR. Three-dimensional overlay culture models of human breast cancer reveal a critical sensitivity to mitogen-activated protein kinase kinase inhibitors. The Journal of pharmacology and experimental therapeutics. 2010; 332:821–8. [PubMed: 19952304]
48. Pickl M, Ries CH. Comparison of 3D and 2D tumor models reveals enhanced HER2 activation in 3D associated with an increased response to trastuzumab. Oncogene. 2009; 28:461–8. [PubMed: 18978815]
49. Moro L, Arbini AA, Yao JL, di Sant'Agnese PA, Marra E, Greco M. Mitochondrial DNA depletion in prostate epithelial cells promotes anoikis resistance and invasion through activation of PI3K/Akt2. Cell death and differentiation. 2009; 16:571–83. [PubMed: 19079138]
50. Hawley SA, Fullerton MD, Ross FA, Schertzer JD, Chevtzoff C, Walker KJ, et al. The ancient drug salicylate directly activates AMP-activated protein kinase. Science. 2012; 336:918–22. [PubMed: 22517326]
51. Kapeller R, Toker A, Cantley LC, Carpenter CL. Phosphoinositide 3-kinase binds constitutively to alpha/beta-tubulin and binds to gamma-tubulin in response to insulin. The Journal of biological chemistry. 1995; 270:25985–91. [PubMed: 7592789]

52. Lee SH, McCormick F. Downregulation of Skp2 and p27/Kip1 synergistically induces apoptosis in T98G glioblastoma cells. Journal of molecular medicine. 2005; 83:296–307. [PubMed: 15605273]

53. Hastak K, Agarwal MK, Mukhtar H, Agarwal ML. Ablation of either p21 or Bax prevents p53-dependent apoptosis induced by green tea polyphenol epigallocatechin-3-gallate. FASEB J. 2005; 19:789–91. [PubMed: 15764647]

54. Qiao M, Iglehart JD, Pardee AB. Metastatic potential of 21T human breast cancer cells depends on Akt/protein kinase B activation. Cancer research. 2007; 67:5293–9. [PubMed: 17545609]

55. Wang X, Michael D, de Murcia G, Oren M. p53 Activation by nitric oxide involves down-regulation of Mdm2. The Journal of biological chemistry. 2002; 277:15697–702. [PubMed: 11867628]

56. Yuen JS, Cockman ME, Sullivan M, Protheroe A, Turner GD, Roberts IS, et al. The VHL tumor suppressor inhibits expression of the IGF1R and its loss induces IGF1R upregulation in human clear cell renal carcinoma. Oncogene. 2007; 26:6499–508. [PubMed: 17486080]

57. Cazanave SC, Elmi NA, Akazawa Y, Bronk SF, Mott JL, Gores GJ. CHOP and AP-1 cooperatively mediate PUMA expression during lipoapoptosis. American journal of physiology Gastrointestinal and liver physiology. 2010; 299:G236–43. [PubMed: 20430872]

58. Iimura M, Nakamura T, Shinozaki S, Iizuka B, Inoue Y, Suzuki S, et al. Bax is downregulated in inflamed colonic mucosa of ulcerative colitis. Gut. 2000; 47:228–35. [PubMed: 10896914]

Statement of Significance

Depletion of Akt2, but not Akt1, induces potent tumor regression in PTEN-deficient prostate cancer xenografts, concomitant with up-regulation of p21 which may serve as a potential biomarker for screening Akt2 activity in clinical samples. The specific role of Akt2 in tumor maintenance provides a rationale for the development of isoform-specific inhibitors for patients with PTEN-deficient cancers.

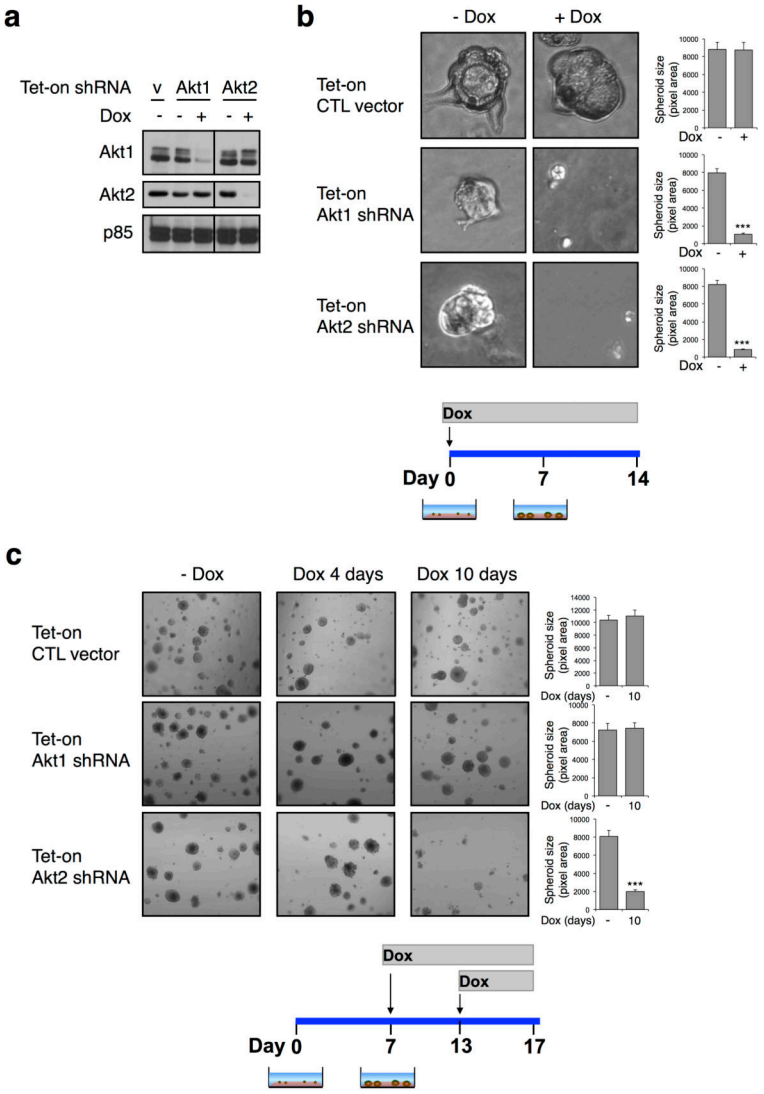

Figure 1. Akt2 silencing induces disintegration of prostate tumor spheroids

A. LNCaP cells expressing tet-on Akt isoform shRNA or vector control (v) were treated with dox (100 ng ml^{-1}) for 2 days. Whole cell lysates were subjected to immunoblotting. **B**. LNCaP cells containing tet-on Akt1 or Akt2 shRNA were grown in 3D culture for 14 days in the presence or absence of dox. Representative phase-contrast images are shown. Spheroid size was quantified in pixel area using Image J and depicted in the bar graph. Error bars represent mean ± standard error of the mean (SEM). ***$P < 0.001$ (Student's *t*-test, $n=30$). **C**. LNCaP cells were cultured in 3D for 7 or 13 days, followed by dox treatment for 10 or 4 days. ***$P < 0.001$ (Student's *t*-test, $n=30$). Spheroid size was quantified in pixel area and depicted in the bar graph. Error bars represent mean ± SEM. ***$P < 0.001$ (Student's *t*-test, $n=30$). Results are representative of at least three independent experiments.

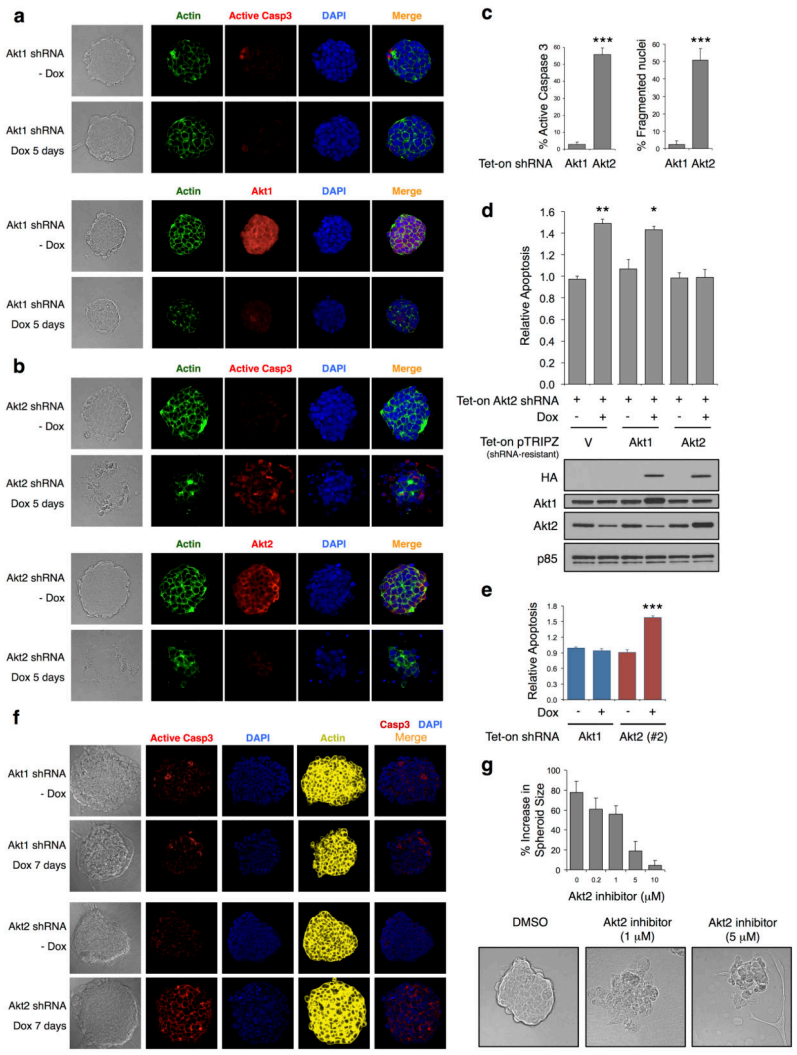

Figure 2. Akt2, but not Akt1, is required for regulating survival of PTEN-deficient prostate tumor spheroids

A. LNCaP cells expressing tet-on Akt1 shRNA were grown in 3D culture for 7 days, followed by dox treatment for 5 days. Immunofluorescence was performed using active caspase 3 (active Casp3) and Akt1 antibodies followed by confocal microscopy. Cell nuclei and actin were labeled with DAPI and Alexa Fluor 488-conjugated phalloidin, respectively. **B**. LNCaP cells expressing tet-on Akt2 shRNA were cultured and stained as in **A**. Akt2 knockdown was confirmed by staining cells with Akt2 antibody. **C**. Percentage of cells containing active caspase 3 and fragmented nuclei was quantified and depicted in the bar graph. Error bars represent mean ± SEM. ***$P < 0.001$ (Student's *t*-test, $n=5$). **D**. LNCaP cells expressing tet-on Akt1 or Akt2 or pTRIPZ control vector were infected with tet-on Akt2 shRNA. Cells were cultured in 3D for 6 days, followed by dox for 8 days. Apoptosis was assessed by staining cells with Annexin V and 7-AAD, followed by FACS analysis. Relative apoptosis was determined by calculating % of annexin-V-positive, apoptotic cells in dox-treated cells relative to the % in mock-treated cells of the same infection. The basal apoptosis levels of pTRIPZ vector-, Akt1 pTRIPZ-, and Akt2 pTRIPZ-infected cells are 25,

23, and 18%, respectively. Error bars represent mean ± SEM. *$P < 0.05$; **$P < 0.01$ (Student's *t*-test, $n=3$). Whole cell lysates were subjected to immunoblotting. **E**. FACS analysis for assessing the effect of an independent Akt2 shRNA (Akt2 #2) on the maintenance of LNCaP spheroids. The basal apoptosis levels of cells expressing tet-on Akt1 and Akt2 shRNA are 33 and 30%, respectively. ***$P < 0.001$ (Student's *t*-test, $n=3$). **F**. PC3 cells expressing tet-on Akt1 or Akt2 shRNA were grown in 3D culture for 6 days, followed by dox treatment for 7 days. Immunofluorescence was performed using active Casp3 antibody followed by confocal microscopy. Cell nuclei and actin were labeled with DAPI and Alexa Fluor 647-conjugated phalloidin, respectively. **G**. Size of LNCaP spheroids grown in 3D culture for 7 days was measured in pixel area using Image J. The spheroids were then treated with the indicated dose of Akt2-selective inhibitor for 48 h. Size of the same spheroids after treatment was measured, and % percentage increase in spheroid size relative to pre-treated spheroids was depicted in a bar graph ($n=8$). Morphology of DMSO and Akt2-selective inhibitor treated spheroids are shown in the phase-contrast images. Results are representative of at least three independent experiments.

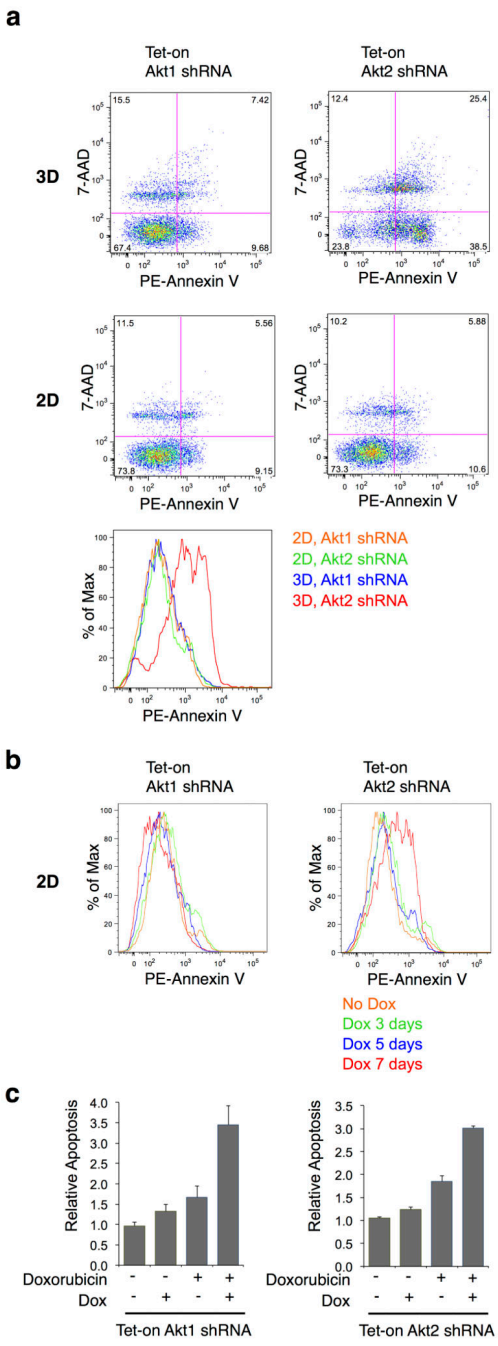

Figure 3. Akt2 depletion has a more profound effect on apoptosis in 3D LNCaP spheroids than in 2D monolayer

A. LNCaP cells expressing tet-on Akt1 or Akt2 shRNA were grown in 2D monolayer or 3D culture for 7 days, followed by dox for 5 days. Apoptosis was assessed by staining cells with Annexin V and 7-AAD, followed by FACS analysis. **B**. LNCaP cells grown in 2D were treated with dox for 3, 5 or 7 days, followed by Annexin V staining and FACS analysis. **C**. LNCaP cells expressing tet-on Akt1 or Akt2 shRNA grown in 2D were treated with dox for 3 days and/or doxorubicin (0.5 μM) for 24 h followed by assessment of apoptosis ($n \geq 3$). The

basal apoptosis levels of cells expressing tet-on Akt1 and Akt2 shRNA are 9 and 18%, respectively. Results are representative of at least three independent experiments.

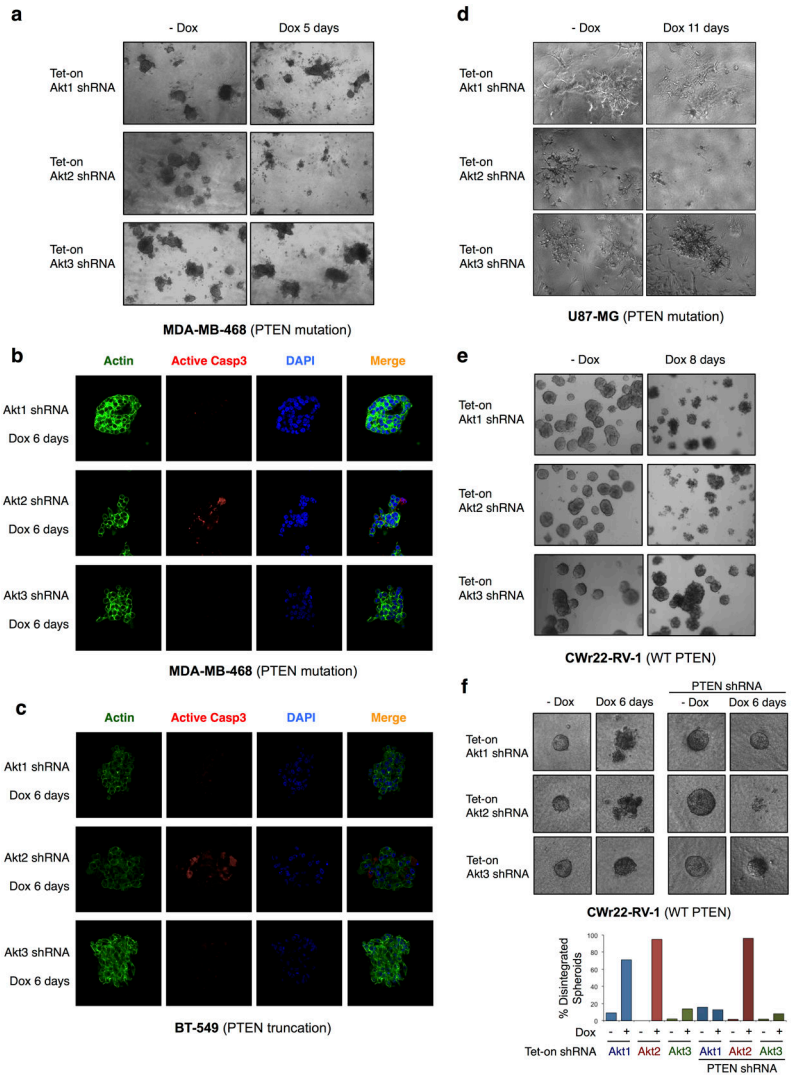

Figure 4. Dependence of PTEN-deficient tumor spheroids on Akt2 for survival

A. MDA-MB-468 cells containing tet-on Akt isoform shRNA were grown in 3D culture for 6 days, followed by dox treatment for 5 days. Representative phase-contrast images are shown. **B**. MDA-MB-468 spheroids were treated with dox for 6 days, followed by staining with active Casp3 and confocal microscopy to assess apoptosis. **C**. BT-549 cells were cultured and stained as in **B. D**. U87-MG cells were cultured in 3D for 7 days, followed by dox treatment for 5 days. Representative phase-contrast images are shown. **E**. CWr22-RV-1 cells containing tet-on Akt isoform shRNA were grown in 3D culture for 7 days, followed by dox treatment for 8 days. **F**. CWr22-RV-1 cells expressing tet-on Akt isoform shRNA were infected with PTEN shRNA. Cells were cultured in 3D for 8 days, followed by dox for 6 days. Percentage of disintegrated spheroids was quantified and depicted in the bar graph ($n \geq 29$). Results are representative of at least three independent experiments.

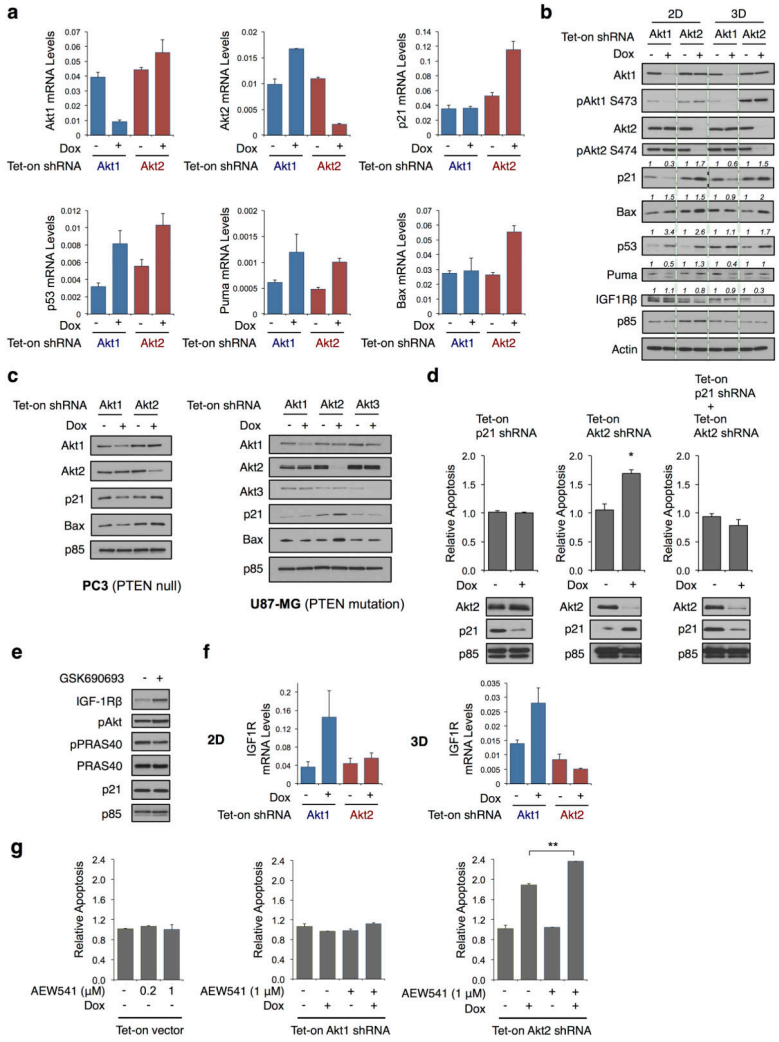

Figure 5. p21 is a critical downstream effector of Akt2 in regulating spheroid maintenance

A. LNCaP spheroids expressing tet-on Akt1 or Akt2 shRNA were treated with dox for 3 days. mRNA levels were analyzed by quantitative real-time RT-PCR. The levels of mRNA are expressed as a ratio relative to the GAPDH mRNA in each sample (*n*=3). B. LNCaP cells expressing tet-on Akt1 or Akt2 shRNA were grown in 2D monolayer or 3D culture for 7 days, followed by dox for 3 days. Protein expressions were analyzed by immunoblotting. Levels of protein expression were quantified and shown as a ratio compared to no-dox control. **C**. PC3 and U87-MG cells expressing tet-on Akt isoform shRNA were treated with dox for 3 days. Lysates were subjected to immunoblot analysis. **D**. LNCaP cells containing tet-on Akt2 and/or p21 shRNA were grown in 3D culture for 8 days, followed by dox for 6 days. Apoptosis was assessed by staining cells with Annexin V and 7-AAD, followed by FACS analysis. The basal apoptosis levels of cells expressing tet-on p21 shRNA, Akt2 shRNA, and (p21 shRNA + Akt2 shRNA) are 36, 24, and 36%, respectively. *$P < 0.05$ (Student's *t*-test, *n*=3). **E**. LNCaP spheroids were treated with GSK690693 (100 nM) for 24 h before harvesting for immunoblot analysis. **F**. LNCaP cells were cultured as in **B**, followed by quantitative real-time RT-PCR (*n*=3). **G**. LNCaP cells containing tet-on vector,

Akt1 or Akt2 shRNA were grown in 3D culture for 8 days, followed by treatment with NVP-AEW541 and/or dox for 7 days. Annexin V-positive cells were assessed by FACS analysis. The basal apoptosis levels of tet-on vector-, Akt1 shRNA-, and Akt2 shRNA-infected cells are 12, 18 and 17%, respectively. $^{**}P < 0.01$ (Student's *t*-test, $n=3$). Results are representative of at least three independent experiments.

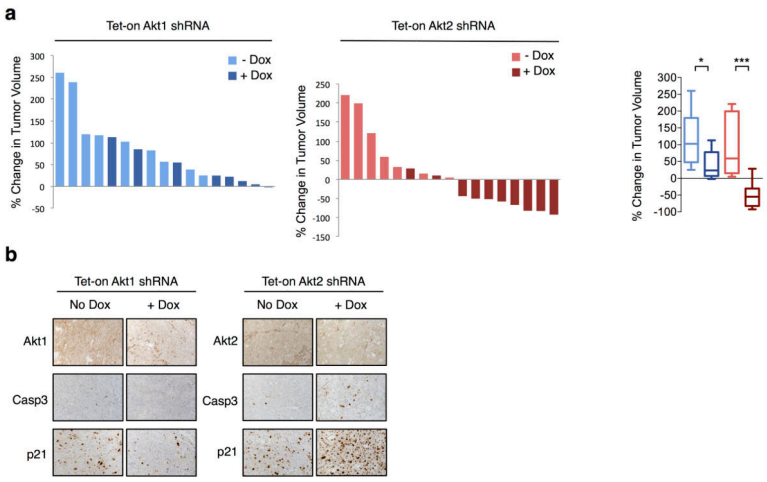

Figure 6. Akt2, but not Akt1, is required for tumor maintenance *in vivo*

A. LNCaP cells expressing tet-on Akt1 or Akt2 shRNA were subcutaneously implanted into nude mice. Mice containing palpable tumors were administered dox (1 mg ml^{-1}) or vehicle control in drinking water for 12 days. Tumor volume was measured by calipering and percentage change in tumor volume was shown in waterfall plots and box-and-whisker graphs. $*P < 0.05$; $***P < 0.001$ (Student's *t*-test, $n \geq 7$). **B**. Akt isoforms, active caspase 3 and p21 immunohistochemistry staining for xenografts in **A**.